# Bond Behavior between Concrete and CFRP Plate under Fatigue Loading

Wei Zhang[1] and Toshiyuki Kanakubo[2]
[1]*Department of Engineering Mechanics and Energy, University of Tsukuba, Tsukuba, Japan*
[2]*Department of Engineering Mechanics and Energy, University of Tsukuba, Tsukuba, Japan*
*E-mail*: wei@rcs.kz.tsukuba.ac.jp

**ABSTRACT:** The experiment by the fatigue loading test for double-face bond specimens is carried out. According to the experiment results to investigate the influence of bond behavior with different concrete strength, types of CFRP plate and variables of upper limit fatigue loading, the fatigue failure of bonding surface between CFRP plates and concrete is finally characterized by the S–N diagram representing the relationship between the upper bond stress and the number of cycles at debonding. The different debonding modes that indicate fracture interface are also observed.

## 1. INTRODUCTION

Rehabilitation or strengthening of existing concrete structures using external attached CFRP (Carbon Fiber-Reinforced Plastic) plate has been developed to extend their life. In these structures, it is frequently necessary not only to augment the strength of beams and slabs that have suffered material deterioration, damage, or an increase of service load, but also to provide sufficient durability to prevent failure from fatigue. Repeated loading can cause the failure by fatigue even if the loading ranges are considerably less than their ultimate capacity. In recently, many studies have reported a variety of CFRP debonding problems. Although the bonding and debonding mechanisms of CFRP sheet under static loading have been quite extensively studied, until now, the study of CFRP plate bond behavior under fatigue loading has rarely been carried out. For strengthening structures, the evaluation of fatigue performances is considered to be a very important one. Based on these considerations, this paper aims at investigating clearly the bond behavior of CFRP plates bonded to concrete under fatigue loading.

## 2. EXPERIMENTAL PROGRAM

### 2.1 Specimens

The prism specimens which size is 150mm ×150mm and 800mm long are used in this experiment. Total 16 specimens are tested. The two steel bars have no connection at the centre of the specimen. Crack is introduced at the notch after attaching CFRP plate. These mean that the two prisms are connected only through the CFRP plates. CFRP plates are bonded at two opposite sides of the specimen. The putty type epoxy adhesive is used for bonding CFRP plate. One of the sides of the specimen was reinforced with confinement CFRP sheet allowing the occurrence of delaminating of the CFRP plate only on the opposite side. The CFRP plate's bond length used for this research was set to 400mm. The CFRP plate width chosen for this research was 50mm for all specimens. The detail of the prism specimen is shown in Fig.1.

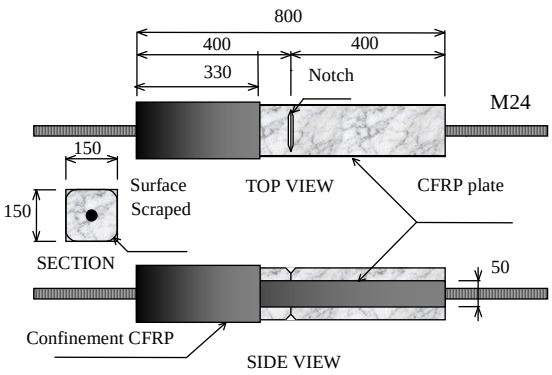


Fig.1. Details of the prism

### 2.2 CFRP Plate and Concrete

CFRP plate's properties are shown in Table 1. The properties of the CFRP plates are values obtained from the manufacturer. Because the main objective of this research is about bond behavior between concrete and CFRP plates under fatigue loading in general, and high strength and high stiffness CFRP plates were used. To verify the influence of bonding behavior, the concrete strength was varied. The actual strength of the concrete is shown in Table 2.

Table 1 CFRP plate properties

| CFRP plate type | Name | Thickness (mm) | Young's modulus (GPa) | Tensile strength (MPa) |
|---|---|---|---|---|
| High strength | GM510 | 1.0 | 156 | 2400 |
| High stiffness | HM520 | 2.0 | 450 | 1200 |

Table 2 Concrete properties

| Concrete Type | Compressive strength (MPa) | 1/3 Secant modulus (GPa) | Splitting strength (MPa) |
|---|---|---|---|
| Target 13.5MPa | 21.2 | 21.4 | 1.96 |
| Target 21MPa | 25.0 | 22.3 | 2.40 |
| Target 36MPa | 39.5 | 24.9 | 3.01 |

### 2.3 Testing Method

In this experiment, a 100t actuator is used for fatigue loading .Total displacement and crack width at the center were measured using linear variable displacement transducers (LVDTs), as shown in Fig.2. The strain distribution was obtained from 9 strain gages set on the CFRP plates on one face (the gage face) at intervals of 50mm, and one gauge on the opposite sides (the no-gage face), at the center of the specimen and the two pi gauges set on the notch. The repetition frequency of cyclic loading is 1 Hz. This frequency was selected because conventional civil engineering structures are typically loaded at frequencies varying between 1 to 5 Hz. And the sinusoidal loading is used to force the specimens.The variables of upper limit fatigue loadings are set as 50%, 60%, 70%, 75%, 80% and 90% of bond strength under static loading $P_{max}$, which is identified as the value among the load carrying capacities investigated by the static test, and the lower limit fatigue loading is set as 10% of $P_{max}$ in all experiments. All of the fatigue loading will up to 1 million cycles if it is not debonding. Table 3 is shown all of the specimens' details.

Full cycles' data recording were taken at the following cycles: at the 1st cycle and every 20th cycle up to 200 cycles, at every 200th cycle up to 1,000 cycles, at the every 1,000th is up to 10,000 cycles, at the

every 10,000th cycle up to 100,000 cycles and at the every 80,000th cycle up to 1,000,000 cycles. The M-series specimens and post fatigue F-series (no-failure by fatigue loading) were tested statically up to failure.

Because the specimen C36HE-F75 failed by concrete splitting and pulling out of the steel bar at the early loading cycle (see Table 4), a concrete confinement jig shown in Fig.3 is set for specimen C21HE-F75-C to prevent splitting failure. Specimen C13HE-M-C is conducted to investigate the influence of the confinement jig under static loading with specimen C13HE-M. As a result, the bond strength of C13HE-M-C was 10% higher than specimen C13HE-M.

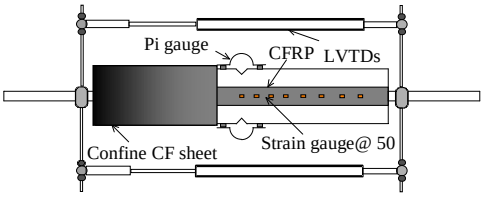


Fig.2. Data acquisition sketch

Table 3 Specimens details

| Specimens | Concrete strength (MPa) | CFRP plate | Fatigue loading | |
|---|---|---|---|---|
| | | | Upper limit | Lower limit |
| C13HS-M | 13.5 | High strength GM510 | Static loading | |
| C13HS-F70 | | | 70% | 10% |
| C13HS-F80 | | | 80% | 10% |
| C13HS-F90 | | | 90% | 10% |
| C13HE-M | | High stiffness HM520 | Static loading | |
| C13HE-M-C | | | | |
| C21HS-M | 21 | High strength GM510 | Static loading | |
| C21HS-F60 | | | 60% | 10% |
| C21HS-F70 | | | 70% | 10% |
| C21HS-F80 | | | 80% | 10% |
| C21HE-M | | High stiffness HM520 | Static loading | |
| C21HE-F75-C | | | 75% | 10% |
| C36HS-M | 36 | High strength GM510 | Static loading | |
| C36HS-F50 | | | 50% | 10% |
| C36HS-F60 | | | 60% | 10% |
| C36HS-F70 | | | 70% | 10% |
| C36HE-M | | High stiffness HM520 | Static loading | |
| C36HE-F75 | | | 75% | 10% |

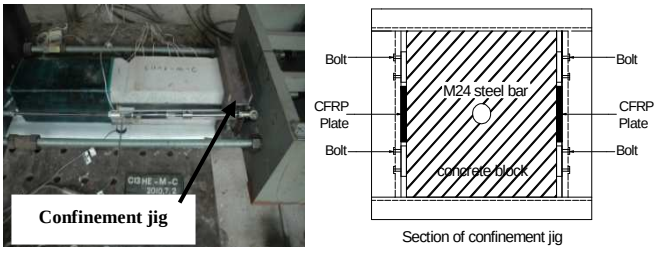


Fig.3. Confinement jig to prevent concrete splitting

## 3. EXPERIMENTAL RESULT

### 3.1 Results under Static Loading

All the seven specimens were submitted to tensile force until total failure of the bond system took place. Under the static loading specimens, some pieces of concrete on the CFRP plate could be found and a layer of concrete was still bonded on the CFRP plate in the specimens after failure. Typical failure in specimens C13HS-M and C13HE-M are shown in Fig.4. The layer of the interface of HE specimens was thicker than HS specimens. All of under static load specimens' failure faces are in concrete face.


Fig.4 Typical failure under static loading

#### 3.1 .1 Load – displacement relationships

The examples of load-crack width at the notch curve of C36HS-M and C36HE-M specimens are shown in Fig.5. The crack width is the average of data from two pi gauges. The crack width of HS specimen at the maximum load is about 0.2mm bigger than the HE specimen. However, the maximum load at failure is much lower than the HE specimen.

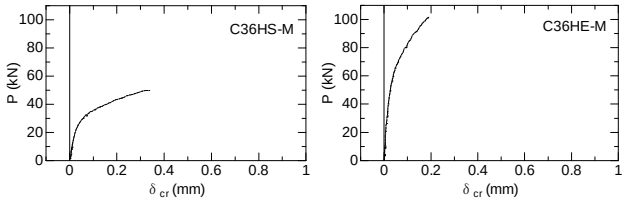


Fig.5 Load-crack width relationship

#### 3.1 .2 Strain distribution

The data obtained from the strain gauges on the CFRP plate was used to create strain versus the distance of the strain gauges from the centre to load end of specimen. Fig.6 shows examples of strain distribution of the specimen C36HS-M and C36HE-M. The certain portion of strain distribution has larger slope, where the active bonding stress exists. It is observed that the local strain of HS specimen is higher than HE specimen; however, the bond strength is lower than HE specimen. Moreover, at the load end, the strain is nearly zero.

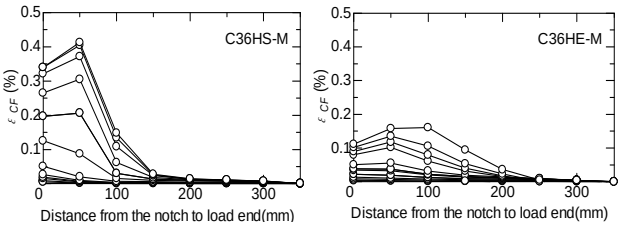


Fig.6 Strain distribution

### 3.2 Results under Fatigue Loading

Eleven specimens were tested under the different upper limit load with fatigue test. The failure progress was that micro-debonding of CFRP plate initiated from the notch and propagated gradually to form macro-debonding. The debonding little by little propagated toward the load end. As the fatigue cycles increased, finally a complete CFRP plate debonding occurred when debonding propagation reached a critical value. The specimens C21HS-F60, C21HE-F75-C and C36HS-F50 were subjected to static loading to failure after 1 million cycles of fatigue loading. In specially, the specimen C36HE-F75 failed at 134 cycles under fatigue loading because of the steel bar pulling out due to concrete splitting. The load versus crack width, the strain distribution of the typical

specimen C21HS-F70 is shown in Fig.7 and Fig.8, respectively. The post-fatigue static response is almost identical to the static response .The typical C21HS-F60 and C21HS-M specimens' $P$-$\delta_{cr}$ curves are shown in Fig.9.

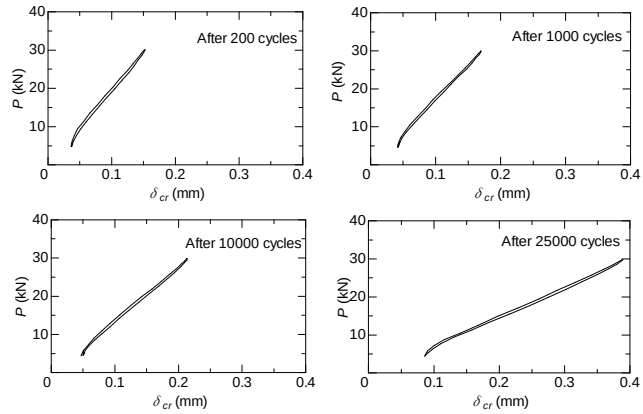


Fig.7 Load-crack width curve of C21HS-F70

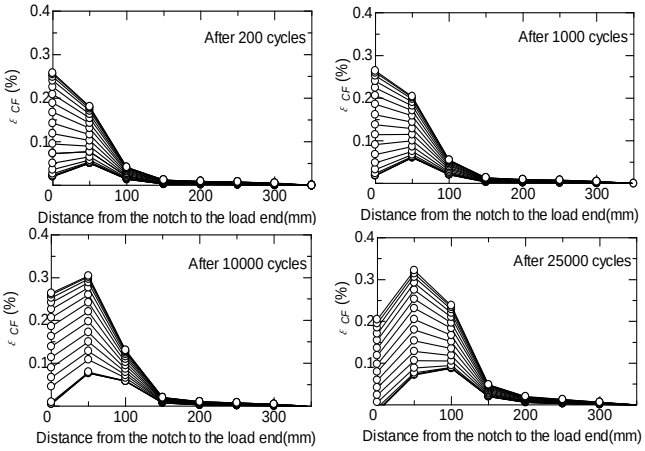


Fig.8 Strain distribution of C21HS-F70

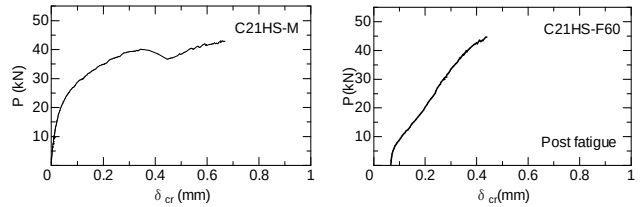


Fig.9 Load-crack width curve by static after fatigue loading

It is observed that as the fatigue cycles increased, the crack width became bigger and bigger as showed in Fig.7. From Fig.8, as the fatigue cycles increased, the maximum local bond stress moved from the notch to load end. Moreover, the maximum strain of CFRP plate moved to the 50mm from notch. That is because at the 50mm from notch where CFRP plate debonding from concrete surface, there was a thicker concrete layer remained on CFRP plate. From Fig.9, post-fatigue static bond strength is almost same to the strength under static loading.

### 3.3 Fatigue Life Prediction

The obtained results suggest a linear relation between the upper limit bond stress $\tau_{up}$ and the logarithm of the number of load cycles to failure $N$ according to the following equation (1) and (2):

$$\tau_{up} = p_{up} / 2b_f l_b \quad \text{.....(1)}$$

$$\tau_{up} = m \cdot \log(N) + n \quad \text{.....(2)}$$

Where, $b_f$ and $l_b$ are CFRP plate width and bond length; $m$ and $n$ are fitting coefficients of experimental data.

The $S$-$N$ curves are shown in Fig.10. The arrows in the figures indicate no failure specimens by 1 million cycles. The fatigue limit to 2 million cycles of specimen C13HS, C21HS and C36HS is expected as 70%, 60% and 50% of bond strength under static loading, respectively. Moreover, with the same type CFRP plate, concrete strength has influence for fatigue life. As concrete strength increased, the fatigue life is prolonged.

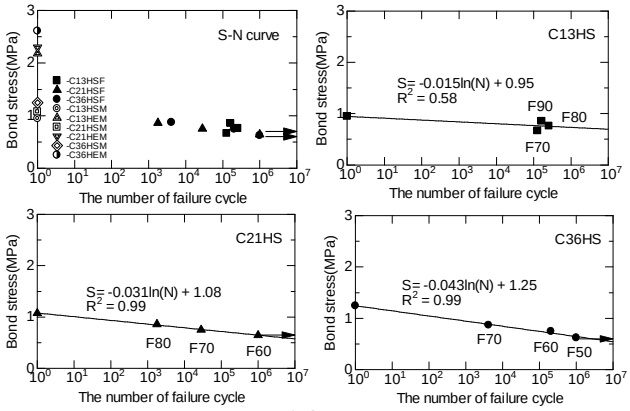


Fig.10 $S$-$N$ curve

### 3.4 Fatigue Failure Mechanism

In this experiment, types of debonding modes due to different upper limit of fatigue loading, types of CFRP plate and concrete strength are observed. All of the fatigue specimens' experimental results are summarized in Table 4 and typical photos are shown in Fig.11. The calculated bond length in Table 4 is calculated by following equations (3) [1].

$$l_e = \sqrt{\frac{2 \cdot \lambda_f \cdot s_e}{k_e}} \quad \text{.....(3)}$$

Where, $l_e$ = effective bond length, $\lambda_f$ = bond length index ($\lambda_f = t_f \cdot E_f / \tau_{b,max}$), $s_e$ = slippage in effective bond length (= 0.234mm), $k_e$ = bond stress ratio in effective bond length (= 0.428), $\tau_{b,max}$ = maximum local bond stress ($\tau_{b,max} = 2.5\sigma_B^{0.23}$), $b_f$ = width of CFRP plate, $t_f$ = thickness of CFRP plate, $E_f$ = elastic modulus of CFRP plate, $\sigma_B$ = concrete compressive strength (in MPa).

Table 4 Fatigue result summarise

| Specimen | Upper limit load $P_{up}$ (kN) | Lower limit load $P_{low}$ (kN) | Calculated bond length $L_e$ (mm) | Upper limit bond stress $\tau_{up}$ (MPa) | Failure cycles |
|---|---|---|---|---|---|
| C13HS-F70 | 26.53 | 3.97 | 184 | 0.663 | 127,445 |
| C13HS-F80 | 30.32 | 3.97 | 184 | 0.758 | 256,819 |
| C13HS-F90 | 34.11 | 3.97 | 184 | 0.853 | 164,012 |
| C21HS-F60 | 25.78 | 4.30 | 180 | 0.645 | No failure* |
| C21HS-F70 | 30.08 | 4.30 | 180 | 0.752 | 28,191 |
| C21HS-F80 | 34.38 | 4.30 | 180 | 0.860 | 1,779 |
| C21HE-F75-C | 68.94 | 9.19 | 433 | 1.724 | No failure* |
| C36HS-F50 | 24.92 | 4.98 | 170 | 0.623 | No failure* |
| C36HS-F60 | 29.90 | 4.98 | 170 | 0.748 | 205,175 |
| C36HS-F70 | 34.89 | 4.98 | 170 | 0.872 | 4,145 |
| C36HE-F75 | 78.35 | 10.45 | 408 | 1.959 | Concrete splitting |

* Up to 1 million cycles

It is observed that the specimen C13HS-F90 failure face is divided into 2 parts. First, debonding occurred from the notch at the concrete surface and propagated to the load end. Second, as fatigue cycles increased, failure face changed to the adhesive face until to CFRP plate completely debonding. The specimen C21HS-F80 failure face

is all at the concrete surface. The specimens C36HS-F70 failure face mechanism is nearly same to the specimen C13HS-F90, just failure face at the concrete surface is less than C13HS-F90. The specimen C36HS-F50 was nothing to happen up to 1 million cycles. And then took static loading to failure. When up to the 1 million cycles, the debonding was almost from the adhesive face. And so, after completely debonding, two parts failure face were observed.


Fatigue cycles are 614,012 | Fatigue cycles are 1,779

Fatigue cycles are 4,145 | Post-Fatigue failures

Fig.11 Fatigue failure surface

### 3.5 Local Bond Stress - Slip Relationship

#### 3.5.1 Calculating of local bond stress and slip [2]

The difference of tensile force of CFRP plate is obtained from the strain of section *i* and section *i*-1. The bond stress of section *i*, $\tau_{b,i}$ is calculated dividing the difference of tensile force by the surface area of the CFRP plate, as shown in Equation (4).

$$\tau_{b,i} = \frac{(\varepsilon_{f,i} - \varepsilon_{f,i-1}) \times t_f \times E_f}{\Delta l_b} \quad \text{.....(4)} \qquad (i = 2-9)$$

Where, $\varepsilon_{f,i}$: strain of CFRP plate of section *i*; $t_f$: thickness of CFRP plate (HS specimen=1mm, HE specimen=2mm); $E_f$: elastic modulus of CFRP plate (as shown in Table 1); $\Delta l_b$: interval between gauges (50mm).

The slip of section *i*, $s_i$, is the sum of the difference between the elongation of CFRP plate and the elongation of the equivalent section compounded of concrete, adhesive layer and steel bar, from the free end of the CFRP plate (= load end of the specimen) to the section *i*. It is assumed that the relative displacement between concrete and CFRP plate at the free end of the CFRP plate is zero. The slip is calculated using the equations (5)-(8) as below.

$$s_i = s_{i-1} + (\delta_{f,i} - \delta_{m,i}) \quad \text{.....(5)} \qquad (i = 2-9,\ s_1 = 0)$$

$$\delta_{f,i} = \frac{\varepsilon_f - \varepsilon_{f,i-1}}{2} \times \Delta l_b + \varepsilon_{f,i-1} \times \Delta l_b \quad \text{.....(6)}$$

$$\delta_{m,i} = \frac{\varepsilon_{m,i-1} - \varepsilon_{m,i}}{2} \times \Delta l_b + \varepsilon_{m,i} \times \Delta l_b \quad \text{....(7)}$$

$$\varepsilon_{m,i} = \frac{P_{m,i-1} - 2 \times \tau_{b,i} \times b \times \Delta l_b}{A_m \times E_m} \quad \text{.....(8)}$$

$$(\varepsilon_{m,1} = P_{m,1} / A_m \times E_m,\ P_{m,1} = P_{load})$$

Where, $\delta_{f,i}$: elongation of CFRP plate in section *i*; $\delta_{m,i}$: elongation of equivalent section *i*; $\varepsilon_{m,i}$: strain of equivalent section *i*; $P_{m,i}$: tensile force acting on equivalent section *i*; $b_f$:width of CFRP plate (50mm); $P_{load}$: tensile force obtained by loading machine; $A_m \cdot E_m$: stiffness of equivalent section.

After calculating all the data, local bond stress versus slip (τ vs. s) graphs for 50-100mm and 100-150mm gauge interval for C21HS-F70 specimen were plotted as shown in Fig. 12.

#### 3.5.2 Local bond stress - slip relationship

Fig. 12 indicates that local bond stress – slip relationship under fatigue loading shows almost elastic manner. However, stiffness of curves becomes smaller as the fatigue loading cycles increase. In the case of 50-100mm portion, maximum bond stress also decreases.

The curves are compared with proposed local bond stress – slip relationship obtained by static loading. The formula is the Popovics model as shown below. [2]

$$\frac{\tau_b}{\tau_{b,\max}} = \frac{s}{s_{\max}} \times \frac{n}{(n-1)+(s/s_{\max})^n} \quad \text{.....(9)}$$

Where, $\tau_{b,max}$: maximum local bond stress; $s_{max}$: slip at $\tau_{b,max}$ ; $n$:constant (=3)

Fig.13 shows graphically results of specimen C21HS-F70 with Popovics model. It may be said that local bond stress – slip relationship under fatigue loading corresponds to a certain portion of hysterisis curve of bond stress – slip relationship.

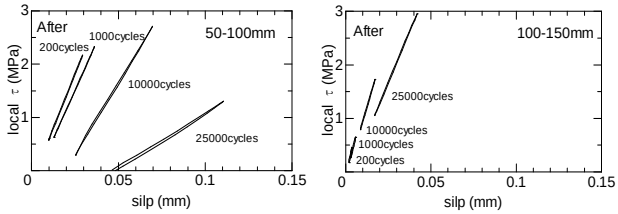


Fig.12 Local τ-s curve of C21HS-F70 specimen

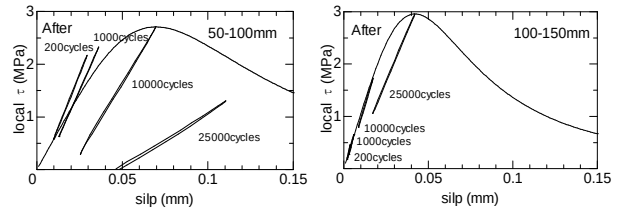


Fig.13 Fitting results by Popovics's equation

## 4. CONCLUSIONS

(1) The fatigue limit to 2 million cycles of bond failure between CFRP plate and concrete is expected as 50%-70% of bond strength under static loading. Moreover, with the same type CFRP plate, concrete strength has influence for fatigue life. As concrete strength increased, fatigue life is prolonged.

(2) Under fatigue loading specimens' failure face include 2 types: 1.Concrete face; 2.First from notch at concrete face and then at epoxy adhesive face.

(3) Local bond stress – slip relationship under fatigue loading shows almost elastic manner. It may be said that local bond stress – slip relationship under fatigue loading corresponds to a certain portion of hysteresis curve of bond stress – slip relationship.

**Acknowledgement**

The authors would like to thank Constec Engi.Co. for their generous contributions for experiments.

## REFERENCES

[1] Matsunaga K., Kanakubo T., et al. "Study on Bond between CFRP Plate and Concrete", Summaries of Technical Papers of Annual Meeting of Architectural Institute of Japan, C-2, 2008, pp.307-310 (in Japanese)

[2] Nakaba K, Kanakubo T, Furuba T, Yoshizawa H. "Bond behaviour between fiber-reinforced polymer laminates and concrete", in ACI Struct J 2001; 98(3):359–67.